R-Ras is required for murine dendritic cell maturation and CD4$^+$ T-cell priming

Gobind Singh,[1] Daigo Hashimoto,[1] Xiaocai Yan,[2] Julie Helft,[1] Patricia J.-Y. Park,[1] Ge Ma,[1] Rui F. Qiao,[1] Colin R. Kennedy,[2] *Shu-Hsia Chen,[1] *Miriam Merad,[1] and *Andrew M. Chan[2]

[1]Department of Oncological Sciences, Mount Sinai School of Medicine, New York, NY; and [2]Department of Pediatrics, Division of Hematology and Oncology, Medical College of Wisconsin, Milwaukee, WI

R-Ras is a member of the *RAS* superfamily of small GTP-binding proteins. The physiologic function of R-Ras has not been fully elucidated. We found that R-Ras is expressed by lymphoid and nonlymphoid tissues and drastically upregulated when bone marrow progenitors are induced to differentiate into dendritic cells (DCs). To address the role of R-Ras in DC functions, we generated a R-Ras–deficient mouse strain. We found that tumors induced in *Rras*$^{-/-}$ mice formed with shorter latency and attained greater tumor volumes. This finding has prompted the investigation of a role for R-Ras in the immune system. Indeed, *Rras*$^{-/-}$ mice were impaired in their ability to prime allogeneic and antigen-specific T-cell responses. *Rras*$^{-/-}$ DCs expressed lower levels of surface MHC class II and CD86 in response to lipopolysaccharide compared with wild-type DCs. This was correlated with a reduced phosphorylation of p38 and Akt. Consistently, R-Ras–GTP level was increased within 10 minutes of lipopolysaccharide stimulation. Furthermore, *Rras*$^{-/-}$ DCs have attenuated capacity to spread on fibronectin and form stable immunologic synapses with T cells. Altogether, these findings provide the first demonstration of a role for R-Ras in cell-mediated immunity and further expand on the complexity of small G-protein signaling in DCs. (*Blood*. 2012; 119(7):1693-1701)

Introduction

Dendritic cells (DCs) are potent antigen-presenting cells with key roles in initiating antigen-specific immune responses.[1] Although numerous reports have implicated members of the *RAS* superfamily of GTP-binding proteins in DC biology,[2] a complete understanding of their individual roles is still lacking. Small GTPases traditionally operate as molecular switches, being inactive in the GDP-bound state and active in the GTP-bound state, therein conferring signaling function through interactions with their downstream effectors.[3] Indeed, several small GTPases have been shown to play critical roles in immune cell functions by regulating actin cytoskeleton-dependent processes.[4-10]

Small GTPases Rap1, Rac1/2, and Cdc42, with the latter 2 being part of the *RHO* family of GTPases, have been demonstrated to be important in DC biology. Active Cdc42 can reactivate endocytosis in mature DCs, whereas microinjection of a dominant negative Cdc42N17 mutant abrogates the uptake of dextran.[9] Interestingly, it was demonstrated in DCs that levels of active Cdc42 and Rac were not increased in response to lipopolysaccharide (LPS).[11] However, using mature DCs from Rac1 and Rac2 double-knockout mice (*Rac1/2*$^{-/-}$), Rac1 and Rac2 were shown to be critical for dendrite formation and T-cell activation.[12] In addition, RAPL, a downstream effector of Rap1, has been shown to be critical for both lymphocyte and DC migration and adhesion.[5,6] Although both Rap1 and Cdc42/Rac GTPases are clearly involved in DC biology, little is known concerning the role of other key members of the Ras subfamily.

R-Ras is a small GTPase that belongs to the Ras subfamily and shares approximately 55% amino acid sequence similarity with the *RAS* proto-oncogenes, *H-RAS*, *N-RAS*, and *K-RAS* (collectively referred to as Ras herein).[13,14] Distinctively, R-Ras possesses a unique 26-amino acid sequence in the amino-terminus that is necessary for Rac activation and Rac-dependent cell spreading.[15] Furthermore, active R-Ras in macrophages has been shown to positively regulate phagocytosis of C3bi-opsonized particles via the integrin M2.[16]

Insights into the physiologic function of R-Ras were revealed through analyzing a mouse strain in which the *R-Ras* gene was disrupted by gene-trap methodology.[17] Here, R-Ras expression was restricted to endothelial and vascular smooth muscle cells, and R-Ras is a negative regulator of vascular proliferation and angiogenesis. Furthermore, these studies suggested that R-Ras has a negligible role in inflammatory responses, as similar levels of F4/80-positive macrophages were seen in atherosclerotic lesions in both wild-type (WT) and R-Ras–deficient mice. More recently, TC21, a closely related small GTPase of R-Ras, has been shown to bind both T- and B-cell antigen receptors and play a role in homeostatic proliferation and survival of these immune cell types.[18]

In this study, we provide evidence of R-Ras expression in multiple murine immune cells that include DCs. Characterization of an *Rras*$^{-/-}$ mouse line revealed multiple defects in DCs, including impaired maturation and T-cell priming, attenuated activation of intracellular signaling pathways downstream of Toll-like Receptor 4 (TLR4), and reduced formation of stable immunologic synapses between DCs and T cells. This report represents the first demonstration of a physiologic function of R-Ras in cell-mediated immune responses.

Submitted May 27, 2011; accepted December 5, 2011. Prepublished online as *Blood* First Edition paper, December 14, 2011; DOI 10.1182/blood-2011-05-357319.

*S.-H.C., M.M., and A.M.C. contributed equally to this study as last co-authors.

The online version of this article contains a data supplement.

The publication costs of this article were defrayed in part by page charge payment. Therefore, and solely to indicate this fact, this article is hereby marked "advertisement" in accordance with 18 USC section 1734.

Methods

Mice

Mice deficient for R-Ras were generated by homologous recombination of ES cells in 129SvEvBrd (129Sv) background by deleting a 1.2-kb region spanning exons 2 to 4 (inGenious Targeting Laboratory). *Rras*$^{+/-}$ mice in a C57BL/6 background were generated by 10 generations of backcrossing. *Rras*$^{-/-}$ mice were obtained by intercrossing *Rras*$^{+/-}$ animals. The genotypes of litters were determined by PCR of genomic DNA with primers specific for WT R-Ras (MRg1, 5′-aaagatctgcactgtggacggcat-3′; MRg2, 5′-ttctccagatctgccttgttccca-3′) and knockout (UNI, 5′-agcgcatcgccttctatcgc-cttc-3′; A4, 5′-cactccccgaggctctaatctcctg-3′) alleles. At an age of 6 to 10 weeks, littermates or age- and sex-matched mice in 129Sv background were used in all experiments, unless otherwise stated. Balb/c and OT-II mice were purchased from The Jackson Laboratory. Mice were maintained under pathogen-free conditions in accordance with Institutional Guidelines, and all mice experiments were approved by the Institutional Animal Care and Use Committee of the Medical College of Wisconsin and the Mount Sinai School of Medicine.

Reagents

A rabbit polyclonal antiserum against the N-terminal 23 amino acid of R-Ras was generated in the author's laboratory. Antibodies for p-Akt Ser473 (clone 587F11, #4051), Akt (#9272), p-p38 Thr180/182 (clone 28B10, #9216), p38 (#9212), p-IκBα Ser32/36 (clone 5A5, #9246), IκBα (#4812), p-Erk1/2 (E10, #9106), and Erk1/2 Thr202/Tyr204 (#9102) were obtained from Cell Signaling Technology. Antibodies for Ras (clone 10, #05-516; Millipore), Rap1 (#610195; BD Biosciences), and Rac (#05–389; Millipore) were purchased from commercial sources. HRP-conjugated anti-actin (#sc-1616), HRP-anti–rabbit IgG (#sc-2313), and HRP-anti–mouse IgG (#sc-2314) were from Santa Cruz Biotechnology. Antibodies for flow cytometric analysis, including phycoerythrin-Cy7 (PE-Cy7)–CD11c, PE-CD86, FITC-MHC class II, and allophycocyanin (APC)–CD40, were obtained from BD Biosciences. Data were collected using a FACS LSR II (BD Biosciences). The following items were from Invitrogen: RPMI 1640 media, FBS, 2mM glutamine, 1% nonessential amino acids, 1% sodium pyruvate, 20mM HEPES buffer, 2-mercaptoethanol, penicillin-streptomycin, and carboxyfluorescein diacetate succinimidyl (CFSE). LPS (*Escherichia coli* 055:B5) and ovalbumin (OVA) were from Sigma-Aldrich.

Tumorigenicity assay

Tumor induction was performed as previously described.[19] Briefly, 10^5 B16-F10 cells were injected subcutaneously in a volume of 100 μL of PBS. Tumor growth was monitored once weekly, and tumor volume was measured with a caliper. Tumor volume was calculated by the formula: $\pi/6$(width × length × height).

BM-DC generation

Primary immature DC cultures were generated by culturing bone marrow precursors for at least 6 days in GM-CSF containing media, with nonadherent cells replated in fresh media every 2 days, as previously described.[20] Maturation was induced by 12-hour treatment with either 0.1 or 1 μg/mL LPS, unless stated otherwise. Splenic DCs (sDCs) were derived from spleens isolated from naive mice and digested in RPMI media containing 10% FBS and collagenase (1 mg/mL) for 30 minutes at 37°C. After digestion, sDCs were isolated using anti-CD11c antibody-coupled magnetic beads, according to the manufacturer's protocol (Miltenyi Biotec). GM-CSF stock vials were kindly provided by Dr Julie Blander (Mt Sinai School of Medicine, New York, NY).

Immunoblotting

DCs were solubilized in RIPA buffer. Protein extracts were subjected to SDS-PAGE on a 12.5% gel. After transferring onto nitrocellulose membranes, filters were blocked in 5% milk in TTBS, and proteins of interest were detected by incubating with primary antibodies overnight, followed by 1-hour incubation with HRP-conjugated secondary antibodies. Bound antibodies were detected by standard ECL detection method (Pierce Chemical) and exposed to radiographic films.

Antigen presentation assay

T-cell depleted splenoctyes (APCs) from *Rras*$^{+/+}$ mice or *Rras*$^{-/-}$ mice (129Sv) were isolated, irradiated (3000 cGy), and used as stimulating cells. T cells (2×10^5) from the spleens of Balb/c mice were isolated by Mouse T-cell Enrichment Columns (R&D Systems) and mixed in triplicates with APCs in different ratios for 4 days. Proliferation was monitored by adding [H^3]-labeled thymidine (1 μCi/well in a 96-well plate) for the last 16 hours. Cells were harvested, and the amount of radioactive materials incorporated was counted in a scintillation counter.

Allogeneic and antigen-specific T-cell assays were performed using Thy1.2$^+$ T cells from naive *Rras*$^{+/+}$ mice purified by AutoMACS (Miltenyi Biotec). For these assays, T cells (2×10^5) were mixed with either bone marrow–derived DCs (BM-DCs) or sDCs in different ratios as indicated for 4 to 5 days. Allogeneic or antigen-specific T-cell proliferation was monitored either by [H^3]-labeled thymidine incorporation or CFSE staining, respectively. For CFSE labeling, freshly isolated T cells (1×10^7 cells/mL) were stained for 10 minutes at 37°C with 10μM CFSE in PBS with 0.1% FBS. Reactions were quenched by the addition of an equal volume of 100% FBS followed by 3 washes in PBS with 10% FBS to ensure complete CFSE removal.

Cell spreading assay

BM-DCs from *Rras*$^{+/+}$ and *Rras*$^{-/-}$ mice were plated at variable concentrations (0.57×10^4, 1.7×10^4, and 5×10^4 cells in 50 μL per well) on fibronectin (10 μg/mL) or BSA-coated 96-well plates. BM-DCs were allowed to attach for 10 to 20 minutes at 37°C. Bright-field images were taken from 5 random fields, and the percentage of spread cells was scored. Similar experiments were performed in 8-well chamber slides (Nalge Nunc) by plating 5×10^3 cells per well in triplicates for immunofluorescence analysis. Briefly, cells were fixed in 3% paraformaldehyde and permeabilized with 0.2% Triton X-100 followed by incubation in Texas Red–conjugated phalloidin (1:500; Invitrogen). For quantifying cell spreading, fluorescence images were first captured with an Axiocam digital camera (Carl Zeiss) using a 20× objective. Round cells lacking membrane protrusions were counted as nonspread cells and used for calculating the percentage of cell spreading. To quantify mean cell length, the maximal width of individual cell was measured by the ruler tool of the ImageJ 1.43 software and expressed as an arbitrary unit. A mean cell length was assigned to each field. For each experimental condition, 9 fields from triplicate wells with an average of 62 cells per field were analyzed.

R-Ras-GTP pull-down assay

For each pull-down reaction, approximately 30 μg of GST-RalGDS-RBD fusion protein was coupled onto 25 μL of glutathione-Sepharose 4B beads (GE Healthcare) as previously described.[21] DCs were solubilized in lysis buffer containing 25mM HEPES-KOH (pH 7.4), 200mM NaCl, 1% NP-40, 2mM EDTA (pH 8.0), 5mM $MgCl_2$, and 0.25% NaDOC. A total of 1 mg of protein lysates was added to loaded beads and incubated for 1 hour at 4°C. Reactions were washed 3 times and boiled in 60 μL of 2× Laemmli buffer.

Microscopy

Differential-interference contrast images (1024 × 1024 pixels) monitoring DC–T-cell interactions were acquired using a 63×/1.4 NA objective, Leica SP5 DMI Inverted Confocal microscope (Leica Microsystems) equipped with a temperature and CO_2 controlled incubation chamber. For these studies, 1×10^4 BM-DCs were activated with LPS (0.1 μg/mL) in high optical grade chambers (Ibidi) for 12 hours. Four hours before beginning image-sequence capture, DCs were loaded with OT-II peptide. During this time, fresh OT-II T cells were purified by antibody depletion (B220$^+$, DX5$^+$, CD8$^+$, CD11b$^+$) from the spleens of naive OT-II mice. Before mixing, DCs and T cells were washed 3 times. Next, 2×10^5 T cells were

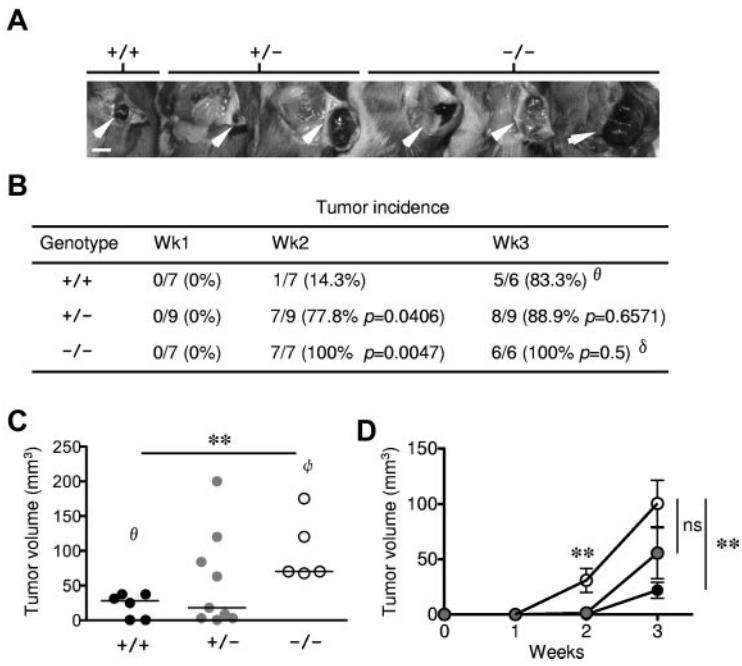

Genotype	Wk1	Wk2	Wk3
+/+	0/7 (0%)	1/7 (14.3%)	5/6 (83.3%) θ
+/−	0/9 (0%)	7/9 (77.8% p=0.0406)	8/9 (88.9% p=0.6571)
−/−	0/7 (0%)	7/7 (100% p=0.0047)	6/6 (100% p=0.5) δ

Figure 1. Enhanced tumor growth in *Rras*$^{-/-}$ mice. (A) Approximately 10^5 B16-F10 cells were injected subcutaneously into *Rras*$^{+/+}$ (n = 7), *Rras*$^{+/-}$ (n = 9), and *Rras*$^{-/-}$ (n = 7) mice in a B6;129Sv genetic background. Images from representative tumors induced after 3 weeks are shown. White arrowheads indicate tumors. Bar represents 0.5 cm. (B) Tumor incidence (%) is shown with the number of animals with palpable tumors indicated. Statistical analysis was performed using Fisher χ^2 (P values). (C) Tumor volumes were measured at week 3. Data derived from 2 independent experiments with 3 to 6 mice each. Bars represent median. $^{**}P < .005$. (D) The kinetics of tumor growth is shown. Bars represent SE. $^{**}P < .005$. ns indicates not significant. θOne *Rras*$^{+/+}$ animal was removed because of mortality. δOne *Rras*$^{-/-}$ animal was removed from incidence analysis because of damaged tumor. ϕTwo *Rras*$^{-/-}$ mice with either tumors that have exceeded humane endpoint (> 2 cm in diameter) or damaged were excluded from tumor volume analysis.

added to the DC-containing chambers. One minute after addition (t = 0), z-stack images were collected on different focal planes for which DC dendrites traversed. This resulted on average one image per focal plane, every 15 seconds for 45 minutes. Videos were generated using Leica Application Suite (Version 1.8.2 build 1465) software, using in-focused images from z-stack accelerated 300×, with the total time length of each video being 5 to 9 seconds. To quantify the number of DC–T-cell contacts, we followed the fate of a single DC along the length of the movie, by scrolling images one by one. Repetitive contacts were scored as 1 interaction, and a DC–T-cell synapse was defined as T-cell in contact with a DC membrane for more than 4 frames (60 seconds). For positive synapses, the time duration of each DC–T-cell synapse was quantified by frame counts as defined earlier in this paragraph. All data shown was collected from 2 randomly selected fields and averaged from 3 independent experiments.

Statistical analysis

Statistical analysis was performed using unpaired Mann-Whitney U test to compare groups of WT and knockout mice. Results are expressed as mean (SE) values. One-tail P value $< .05$ is considered statistically significant.

Results

Generation of *Rras*$^{-/-}$ mouse strain

To address the physiologic role of R-Ras, *Rras*$^{-/-}$ mice were generated by homologous recombination, deleting an intragenic 1.2-kbp region. This region spans exons 2 to 4, which included the switch I and II regions encompassing amino acids 52 to 151 (supplemental Figure 1A, available on the *Blood* Web site; see the Supplemental Materials link at the top of the online article). Intragenic deletion of R-Ras was confirmed by Southern blotting and PCR-based analysis of genomic DNAs (supplemental Figure 1B-C). The lack of R-Ras expression was revealed by Western blotting analysis (supplemental Figure 1D). Similar to a previous report,[17] *Rras*$^{-/-}$ mice generated in this study have the predicted Mendelian ratio of inheritance and lacked gross morphologic aberrations. In addition, *Rras*$^{-/-}$ mice in both 129Sv or C57BL/6 genetic background showed no significant defects in T-cell development in the thymus or in CD11c$^+$, B220$^+$, CD8$^+$, or CD4$^+$ cells in the spleen (data not shown).

Enhanced tumor growth in *Rras*$^{-/-}$ mice

Previous studies have uncovered a lack of R-Ras expression in epithelial cells but readily detectable in various stromal cell types.[17] As an initial attempt to evaluate the physiologic responses to exogenously introduced tumor, 1×10^5 B16-F10 (C57BL/6 background) mouse melanoma cells were injected subcutaneously in *Rras*$^{-/-}$ mice of mixed B6;129Sv genetic background. By week 2, tumor incidence in *Rras*$^{-/-}$ (100%) and *Rras*$^{+/-}$ (77.8%) mice was significantly higher than in *Rras*$^{+/+}$ (14.3%) mice (Figure 1A-B). The mean volume of B16-F10 tumors induced in *Rras*$^{-/-}$ mice ($30.9 \pm 10.9\ mm^3$) was significantly greater than in *Rras*$^{+/-}$ mice ($1.5 \pm 0.6\ mm^3$). By week 3, almost all mice have palpable tumors. However, the mean tumor volume induced in *Rras*$^{-/-}$ mice ($100.5 \pm 21.1\ mm^3$) was approximately 5-fold and approximately 2-fold greater than in *Rras*$^{+/+}$ ($21.9 \pm 7.2\ mm^3$) and *Rras*$^{+/-}$ ($55.6 \pm 22.9\ mm^3$) mice, respectively (Figure 1C-D). In addition, several *Rras*$^{+/-}$ mice possessed tumors of similar size as in *Rras*$^{-/-}$ mice, suggesting dose dependency on the observed phenotypic differences (Figure 1C). These data were in contrast with those obtained from Komatsu and Ruoslahti,[17] where they have not observed differences in tumor incidence and sizes using F3 to F5 mice backcrossed to a C57BL/6 background. These differences may be attributed to the fact that we injected 5 times less cells and animals of B6;129Sv genetic background were used instead. Although these results do not necessarily identify the involvement of immune cells, defects in DCs are known to subvert tumor immune surveillance.[22] Furthermore, the fact that less was known concerning R-Ras in the immune system has prompted us to investigate the role of this Ras-related protein in immune cells.

R-Ras expression in immune cells

To characterize the role of R-Ras in the immune system, its expression in both lymphoid and nonlymphoid tissues was examined. Previous studies have uncovered R-Ras expression restricted

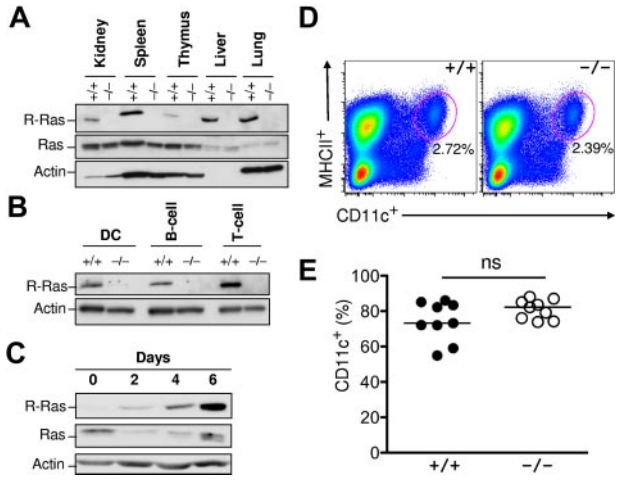

Figure 2. R-Ras expression in immune cells. (A) WT (+/+) and R-Ras knockout (−/−) organs were isolated, and total cell extracts were subjected to Western blotting analysis with the indicated antibodies. (B) WT (+/+) and R-Ras knockout (−/−) spleen was dissociated and subjected to cell sorting with DC-, B cell–, and T cell–specific markers. Western blotting analysis was carried out using an R-Ras specific antibody. (C) Bone marrow progenitors from 6- to 8-week-old mice were cultured in the presence of GM-CSF for 6 days. Cells were monitored throughout the DC differentiation process for R-Ras expression by Western blotting. Parallel membranes were probed with an anti–Ras monoclonal antibody (Millipore). Actin was used as a protein loading control. (D) Age-matched spleens from *Rras*$^{+/+}$ and *Rras*$^{-/-}$ mice were harvested and analyzed for the percentage of MHC class II^{+}CD11c^{+} DCs. (E) Day 6 BM-DC cultures from *Rras*$^{+/+}$ (n = 9) and *Rras*$^{-/-}$ (n = 9) mice were analyzed for the percentage of CD11c^{+} DCs. ns indicates not significant. Results are representative of 3 independent experiments.

to the lung, spleen, and intestine but almost undetectable in the bone marrow.[17] As shown in Figure 2A, R-Ras was readily detected in the lung, as previously reported in addition to the spleen, liver, and kidney. Low levels of expression were observed in primary lymphoid organs, such as the thymus (Figure 2A). Next, splenic B220^{+} B cells, CD3^{+} T cells, and CD11c^{+} DCs from *Rras*$^{+/+}$ and *Rras*$^{-/-}$ mice were isolated with more than 99% purity by FACS and analyzed for R-Ras expression by Western blotting analysis. DCs isolated from *Rras*$^{+/+}$ mice expressed an approximately 23-kDa protein species that was absent in *Rras*$^{-/-}$ cells (Figure 2B). A similar expression pattern was also observed for both B cells and T cells. To validate R-Ras expression in DCs, BM-DCs were cultured in the presence of GM-CSF. From day 0 to day 6, R-Ras levels progressively increased more than 20-fold during differentiation (Figure 2C). On the contrary, the levels of the prototypic Ras proteins were reduced. However, this drastic increase in R-Ras expression was unlikely to play a role in DC development in vivo as *Rras*$^{+/+}$ and *Rras*$^{-/-}$ mice had similar percentages of splenic resident MHC class II^{+}CD11c^{+} DCs (Figure 2D). In addition, there were no differences in the percentage of CD11c^{+} in day 6 BM-DC cultures from *Rras*$^{+/+}$ and *Rras*$^{-/-}$ mice (Figure 2E).

R-Ras controls the ability of DC to activate allogeneic T cells

The observed expression of R-Ras in DCs and lymphocytes has prompted us to examine potential defects in immune response in *Rras*$^{-/-}$ mice. To determine whether *Rras*$^{-/-}$ DCs are defective in their ability to prime naive T cells, irradiated *Rras*$^{+/+}$ and *Rras*$^{-/-}$ splenic cells were cocultured with allogeneic Balb/c T cells for 4 days. T-cell proliferation was significantly reduced by more than 70% when allogeneic T cells were cocultured with *Rras*$^{-/-}$ splenocytes when compared with *Rras*$^{+/+}$ cells (Figure 3A). Similar T-cell proliferation assays were performed using LPS-activated splenic DCs from *Rras*$^{+/+}$ and *Rras*$^{-/-}$ mice. As expected, the ability of *Rras*$^{-/-}$ DCs in stimulating T-cell proliferation was impaired by 25% to 45% compared with *Rras*$^{+/+}$ DCs (Figure 3B). These results were further validated by mixing similar numbers of *Rras*$^{-/-}$ BM-DCs (129Sv) with Balb/c T cells. In this case, the ability of *Rras*$^{-/-}$ BM-DCs to stimulate T-cell proliferation was decreased by 62% to 89% compared with *Rras*$^{+/+}$ (Figure 3C). These data suggest that R-Ras plays a role in mounting an allogeneic response.

R-Ras controls the ability of DCs to prime antigen-specific T cells

To further study the role of R-Ras in T-cell priming, ex vivo antigen specific T-cell responses were assayed. To this end, *Rras*$^{+/+}$ or *Rras*$^{-/-}$ mice were injected intraperitoneally with PBS, LPS, or LPS plus OVA to allow for efficient DC maturation and loading with OVA antigen. Subsequently, splenic DCs were isolated and cocultured with CFSE-labeled polyclonal syngeneic T cells isolated from naive *Rras*$^{+/+}$ mice. Consistent with a reduced capacity in activating allogeneic T cells, splenic DCs isolated from *Rras*$^{-/-}$ mice injected with LPS and OVA were approximately 73% less effective in priming a T-cell response (Figure 3D-E). These data establish that R-Ras expression in DCs is necessary for the priming of allogeneic and antigen-specific autologous responses.

Impaired LPS induced DC maturation in *Rras*$^{-/-}$ DCs

The observed defects in T-cell priming led us to further explore the role of R-Ras in additional DC functions. DC maturation is critical for mounting an efficient T-cell response. To examine the role of R-Ras in DC maturation, the levels of CD86 and MHC

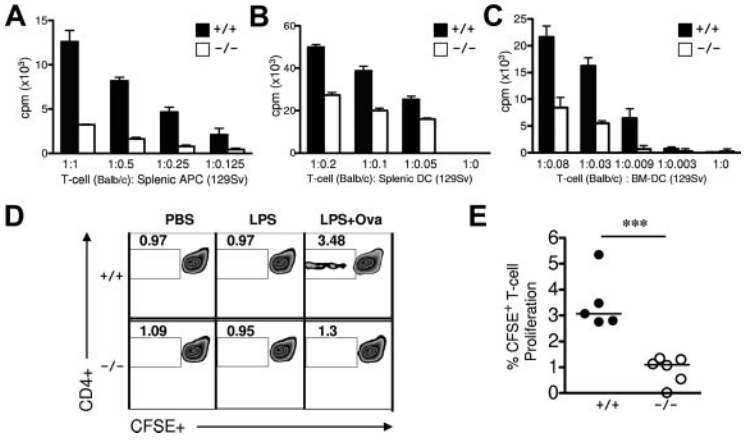

Figure 3. Rras$^{-/-}$ splenic APCs and BM-DCs show impaired T-cell proliferation capacity. (A) Bulk splenic APCs (129Sv; n = 3) or (B) splenic DCs (129Sv; n = 4) from *Rras*$^{+/+}$ or *Rras*$^{-/-}$ mice in different ratios were comixed with 2 × 10^{5} T cells from WT Balb/c for 96 hours. Allogeneic T-cell proliferation was measured by adding [H^{3}]-labeled thymidine for the last 16 hours, and the amount of incorporation was measured by a scintillation counter. Results represent triplicate measurements from a single experiment with data in panel A reproduced in 2 additional experiments. (C) A similar proliferation assay using WT T cells was conducted as in panels A and B, except that BM-DCs (129Sv) were used. Bars represent SD. (D) In vivo T-cell proliferation assays were performed. *Rras*$^{+/+}$ or *Rras*$^{-/-}$ mice (129Sv) were injected intraperitoneally with PBS, 10 μg LPS, or 10 μg LPS and 1 mg OVA. Six hours after injection, splenic DCs were isolated and comixed with naive CFSE-labeled polyclonal syngeneic splenic T cells (129Sv) for 96 hours. CFSE^{+} staining was analyzed by flow cytometry to measure T-cell proliferation. All plots are gated for TCR^{+}CD4^{+} cells. (E) Percentages from panel D for CFSE^{+} proliferating T cells are plotted. Results represent data from 2 independent experiments with *Rras*$^{+/+}$ (n = 5) and *Rras*$^{-/-}$ (n = 6) mice. Bars represent median. ***$P < .0005$.

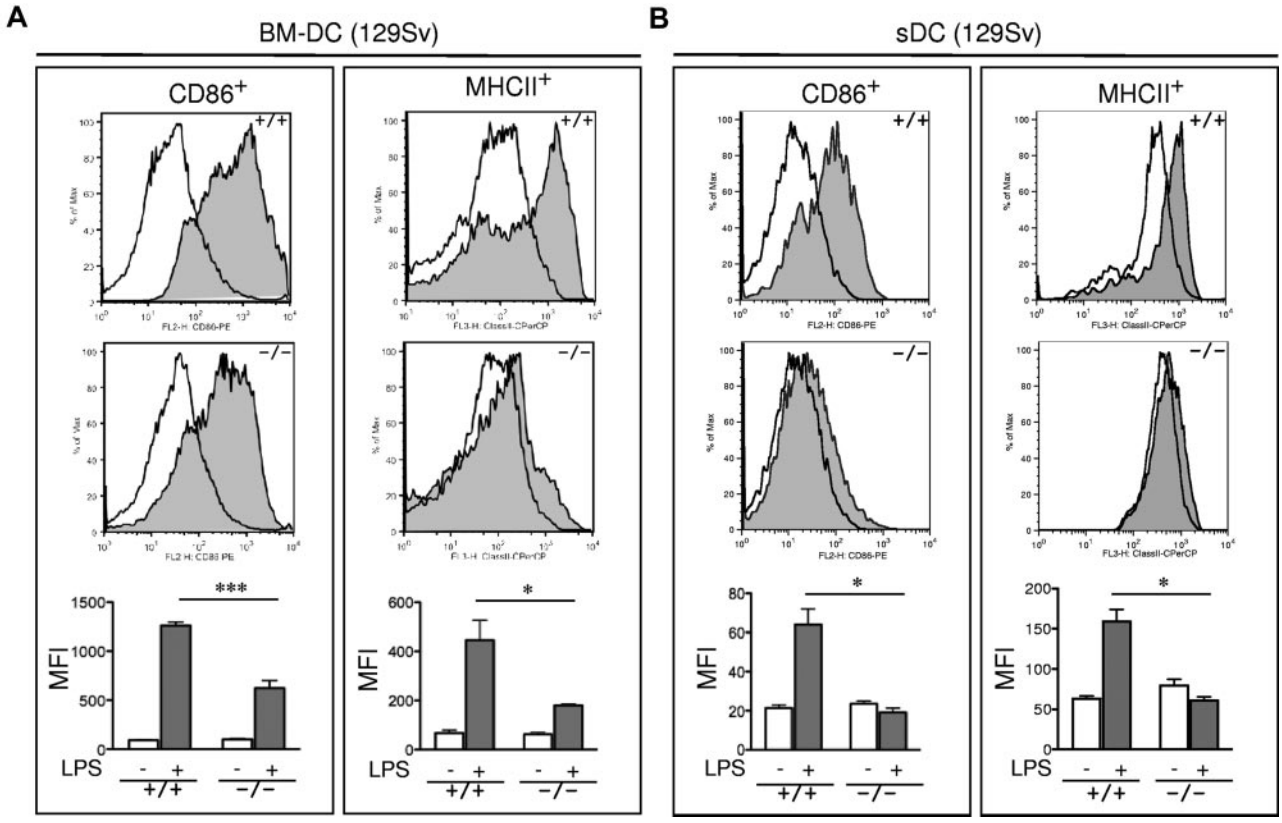

Figure 4. Impaired maturation of *Rras*$^{-/-}$ BM-DC. (A) BM-DCs in culture for 6 days from *Rras*$^{+/+}$ (n = 3) and *Rras*$^{-/-}$ mice (n = 3) in 129Sv strain were treated without (opened areas) or with (shaded areas) LPS (0.1 μg/mL) for 12 hours. Maturation markers were plotted as histograms on CD11c^{+} gated cells. MFI values are quantified in the bottom panels. Bars represent SE. ***$P < .0005$. *$P < .05$. Similar results were reproduced in an independent experiment (supplemental Figure 3A). (B) *Rras*$^{+/+}$ (n = 3) and *Rras*$^{-/-}$ (n = 3) mice were intraperitoneally injected with 10 μg LPS (0.45 mg/kg). After 6 to 8 hours, the levels of maturation markers were analyzed on CD11c^{+} gated cells as described in panel A. Bars represent SE. *$P < .05$. Similar results were obtained in at least 2 independent experiments (supplemental Figure 3C).

class II after LPS stimulation were compared between BM-DCs derived from *Rras*$^{+/+}$ or *Rras*$^{-/-}$ mice. As shown in Figure 4A, unstimulated *Rras*$^{+/+}$ and *Rras*$^{-/-}$ BM-DCs showed low levels of CD86 and MHC class II. Exposure to 0.1 μg/mL of LPS increased surface expression of both CD86 and MHC class II in *Rras*$^{+/+}$ DCs. In contrast, the surface expression levels of CD86 and MHC class II were significantly reduced in *Rras*$^{-/-}$ DCs by 50.6% and 59.6%, respectively (Figure 4A; supplemental Figure 3A). This defect was observed over a broad range of LPS concentrations from 0.001 to 1 μg/mL (supplemental Figure 2A). These differences were unlikely the result of reduced TLR4 expression in *Rras*$^{-/-}$ mice as FACS analysis revealed comparable expression with that of *Rras*$^{+/+}$ mice (supplemental Figure 2B). In addition, similar defects in up-regulating surface CD86 and MHC class II were observed in BM-DCs isolated from mice in C57BL/6 genetic background (supplemental Figure 3B). In addition, *Rras*$^{-/-}$ BM-DCs also displayed attenuated up-regulation of maturation markers when stimulated with other TLR ligands, such as CpG, polyIC, and flagellin (supplemental Figure 4). These findings suggest that R-Ras may mediate the signaling events emanated from different TLRs. Consistently, on systemic LPS injection, *Rras*$^{+/+}$ splenic DCs have increased CD86 and MHC class II expression compared with untreated controls, whereas *Rras*$^{-/-}$ splenic DCs showed significant decreases in these maturation events (Figure 4B). The impaired maturation seen in BM-DCs and splenic DCs demonstrates that R-Ras is required for DC maturation, and this may account for the defects in T-cell priming observed in *Rras*$^{-/-}$ mice.

R-Ras is required for TLR4 signaling

Results in Figure 4 suggest that R-Ras controls the ability of DCs to respond to TLR activation. To test whether R-Ras was activated in response to TLR4 activation, the kinetics of R-Ras activation were monitored by affinity pull-down assays using the Ras binding domain of Ral-GDS (RalGDS-RBD) as a probe that could bind the active form of R-Ras. As demonstrated in Figure 5A, the levels of R-Ras-GTP were increased by approximately 3.5-fold within 10 minutes of LPS stimulation and returned to basal levels by 6 hours. This magnitude of change in GTP loading was commonly observed for R-Ras, as has been shown in semaphorin4D-treated primary neurons.[23] Similarly, Rap1 was maximally activated by LPS by 10 minutes but distinct from R-Ras in having a biphasic activation profile. On the contrary, the prototypic Ras proteins were not activated to an appreciable level until 1 hour after LPS addition (Figure 5A). These findings demonstrate that R-Ras can be acutely activated in response to TLR4 stimulation.

To further delineate the relevance of R-Ras in the downstream signaling of TLR4, the activation states of several key signaling kinases in *Rras*$^{+/+}$ and *Rras*$^{-/-}$ BM-DCs were examined. In *Rras*$^{+/+}$ DCs, a biphasic response for Akt activation was observed with robust activation within 5 minutes and less so after 6 hours of TLR4 stimulation (Figure 5B). Under similar conditions, the magnitude of Akt activation in *Rras*$^{-/-}$ DCs was reduced by approximately 5-fold and the biphasic response was not appreciable. The PI3K/Akt pathway has been shown to positively regulate DC activation through NF-κB and p38.[24] On TLR4

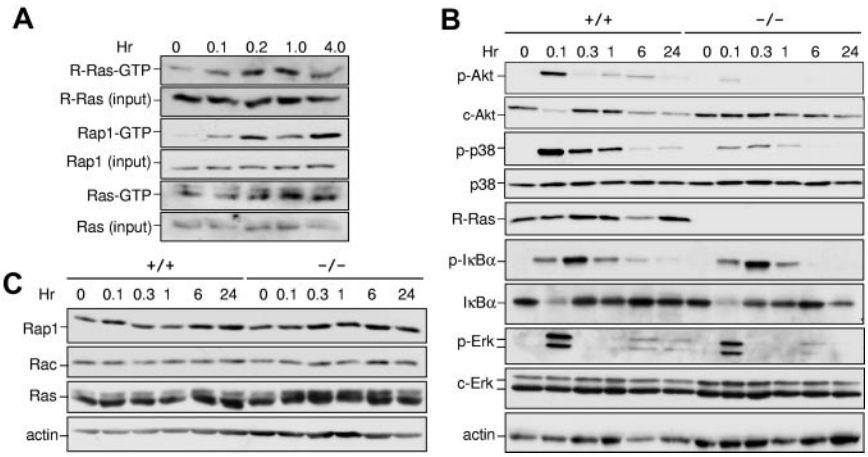

Figure 5. Impaired signaling in *Rras*$^{-/-}$ BM-DCs. (A) *Rras*$^{+/+}$ BM-DCs were exposed to LPS (1 μg/mL) for the indicated duration, and the levels of GTP-bound R-Ras were measured by an affinity pull-down assay using GST-RalGDS-RBD as a probe. The total levels of R-Ras in the corresponding lysates were detected using an anti–R-Ras specific antibody. Similar experiments were performed for Rap1 and Ras using GST-RalGDS-RBD and GST-Raf-RBD as probes, respectively. (B-C) BM-DCs were treated with LPS (1 μg/mL) for the indicated duration, and total cell lysates were prepared. Western blotting analysis was carried out using the indicated antibodies. Similar results were obtained from 2 additional experiments.

stimulation, *Rras*$^{+/+}$ DCs displayed robust activation of p38 and IκBα that peaked at 6 and 18 minutes, respectively, followed by their down-modulation (Figure 5B). In contrast, *Rras*$^{-/-}$ DCs activated with LPS displayed an approximately 7-fold decrease in p38 activation. However, no significant differences were observed in IκBα or ERK1/2 activation (Figure 5B). Furthermore, there were no drastic changes in the levels of other related small GTPases, such as Rap1, Rac, and Ras (Figure 5C). Together, these data implicate R-Ras as a mediator of TLR4 signaling through Akt and p38 MAPK.

Rras$^{-/-}$ DCs are impaired in forming T-cell synapses

Dynamic changes in actin cytoskeleton regulate DCs ability to form immune synapses with T cells. These complex processes are coordinated by small GTPases of the Ras and Rho subfamilies.[25,26] Indeed, defects in Wiscott-Aldrich syndrome are attributed to failure of the Rho family of small GTPases to coordinate actin cytoskeleton in DCs, resulting in reduced cellular protrusions.[27,28] In light of the observed defects in DC maturation and previous data suggesting R-Ras being upstream of Rac and Rap1,[16,29-31] it was possible that R-Ras may play a role in actin cytoskeletal rearrangement in DCs.

The ability to spread on defined extracellular matrix is indicative of a dynamic actin cytoskeleton. To study the role of R-Ras in DC spreading, the relative ability of *Rras*$^{+/+}$ and *Rras*$^{-/-}$ DCs to spread on fibronectin was compared. For this, BM-DCs cultured in vitro for 6 days were used. Within 20 minutes of plating, spreading was evidenced in *Rras*$^{+/+}$ DCs with the formation of the characteristic stellate morphology (Figure 6A). In contrast, *Rras*$^{-/-}$ DCs retained a mostly rounded morphology with an approximately 75% decrease in cell spreading (Figure 6B). To test whether similar observations could be detected in DCs propagated for longer time, BM-DCs cultured for 9 days were also examined. For these experiments, the actin cytoskeletal structures were analyzed by staining with phalloidin. Overall, these cultures harbored greater propensity to spread on either BSA- or fibronectin-coated wells, with more than 40% of cell spreading (Figure 6D). Intense staining

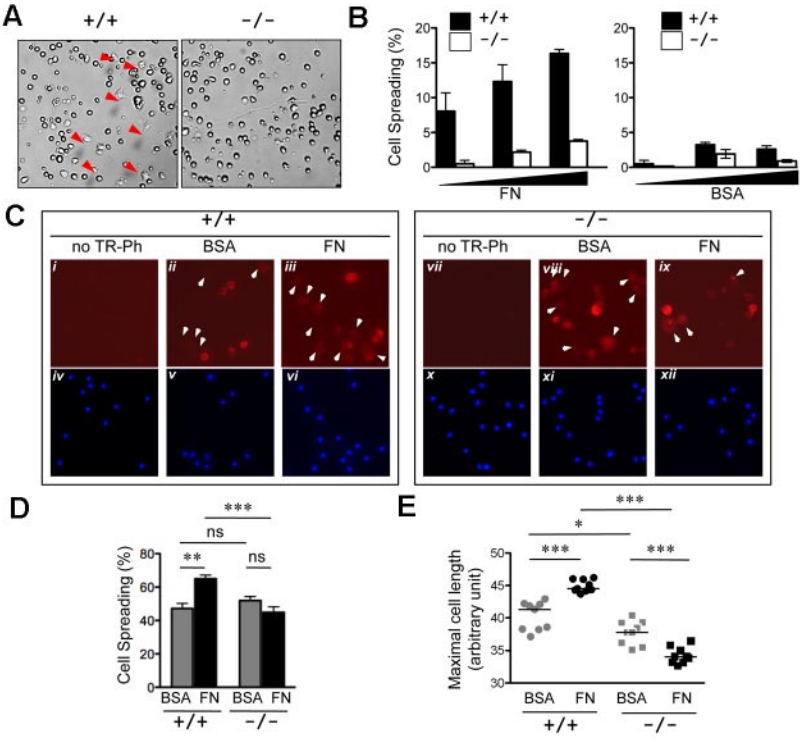

Figure 6. Attenuated cell spreading in *Rras*$^{-/-}$ DCs. (A) Day 6 BM-DCs from *Rras*$^{+/+}$ (n = 1) or *Rras*$^{-/-}$ (n = 1) mice were plated on fibronectin (FN; 10 μg/mL) or BSA-coated plates and allowed to attach for 20 minutes. Images were taken from 5 random fields, and the percentage of spread cells (red arrows) was scored. (B) Results are from a single experiment using increased concentrations (▲) of BM-DCs and have been repeated once with similar results. Bars represent SD. (C) Immunofluorescence analysis of day 9 *Rras*$^{+/+}$ (n = 1) or *Rras*$^{-/-}$ (n = 1) BM-DCs using Texas Red-conjugated phalloidin (TR-Ph; ii-iii,viii-ix, red) to stain F-actin filaments. Cell nuclei were visualized by 4,6-diamidino-2-phenylindole (iv-vi,x-xii, blue). Arrowhead indicates spread cells. (D) The percentages of spread cells were quantified as described in "Cell spreading assay." ns indicates not significant. (E) The maximal cell length was determined by ImageJ software, with each data point representing the mean cell length for a single field of approximately 62 cells. (C-E) Results were from a single experiment, and 9 fields were selected from triplicate wells with an average of 550 cells being analyzed per group. Bars represent SE. ***$P < .0005$. **$P < .005$. *$P < .05$.

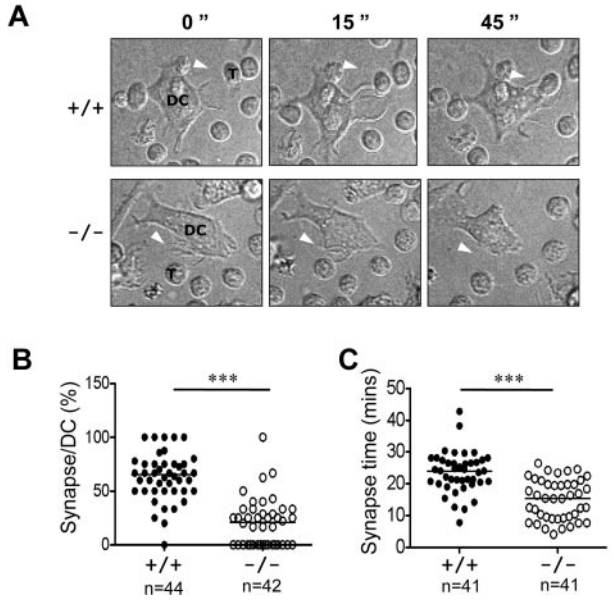

Figure 7. Attenuated immune synapse formation in *Rras*$^{-/-}$ DCs. (A) Time-lapse confocal images at different time points are shown, illustrating an example of a synapse between a mature *Rras*$^{+/+}$ or *Rras*$^{-/-}$ DCs with a naive T cell. White arrows indicate DC protrusions. DCs and T cells (T) are indicated. (B) The percentage of DC–T-cell synapses were quantified ($n > 40$ for each genotype) as described in "Microscopy." (C) The duration (minutes) of T-cell synapses ($n = 41$) with either WT- or KO-activated DCs was quantified. ***$P < .0005$. Bars represent median.

of cortical actin structure was evidenced in rounded *Rras*$^{+/+}$ BM-DCs plated on BSA (Figure 6Cii). Plating on fibronectin induced a modest but significant 37.7% increase in the number of cells with elongated morphology (Figure 6Ciii,D). On the contrary, the extent of cell spreading was not altered for *Rras*$^{-/-}$ BM-DCs plated either on BSA or fibronectin (Figure 6Cviii-ix,D). More important, the extent of cell spreading on fibronectin was significantly higher for *Rras*$^{+/+}$ BM-DCs compared with *Rras*$^{-/-}$ (Figure 6D). As an independent mean to assess cell spreading, the mean cell length was determined. As shown in Figure 6E, plating on fibronectin significantly increased the mean cell length of *Rras*$^{+/+}$ BM-DCs. On the contrary, *Rras*$^{-/-}$ BM-DCs have reduced cell size, and fibronectin did not stimulate an increase in mean cell length.

DCs undergo significant actin reorganization during maturation, therein projecting long and motile membrane extensions. These processes are necessary for DCs to form stable interactions with T cells during priming.[32] We used time-lapse video microscopy to visualize synapses between antigen-loaded mature DCs and naive antigen-specific TCR transgenic T cells. Whereas immature *Rras*$^{+/+}$ and *Rras*$^{-/-}$ DCs did not display dendritic protrusions and migrated slowly, LPS efficiently stimulated peripheral extensions and the acquisition of a stellate morphology (Figure 7A; supplemental Videos 1-4). In addition, increased DC migration distances were observed. The dendrites on mature DCs would actively capture T cells with the formation of multiple synapses (supplemental Video 3). Consistent with previous findings, the percentage of synapses observed between mature *Rras*$^{+/+}$ DCs and naive T cells was measured to be 62.9% ± 21.9% (Figure 7B).[12] In contrast, the percentage of *Rras*$^{-/-}$ DCs forming stable synapse was significantly decreased, reaching only 20.5% ± 22.3%. Analysis of individual positive synaptic events revealed an average interaction duration of 23.6 ± 6.5 minutes for *Rras*$^{+/+}$ DCs and 15.0 ± 6.3 minutes for *Rras*$^{-/-}$ DCs (Figure 7C). Furthermore, although mature DCs migrated more than immature DCs, differences in total distance traveled were noted between mature *Rras*$^{+/+}$ and *Rras*$^{-/-}$ DCs (data not shown), consistent with the observation that *Rras*$^{-/-}$ DCs were defective in maturation. Taken together, these results demonstrate the importance of R-Ras in DC function that can be attributed to a failure in establishing stable immune synapse with T cells.

Discussion

In this study, we characterized an R-Ras knockout mouse strain for defects in immune responses. Our results represent the first demonstration of the ability of R-Ras in controlling DC maturation in response to TLR4 ligand. Consistently, *Rras*$^{-/-}$ DCs are impaired in their ability to prime allogeneic and antigen specific T cells and compromised in forming stable immunologic synapses with antigen specific T cells.

Our findings are reminiscent of CD4^{+} T-cell priming defects observed in *Mindin*-null mice that are associated with a reduction in Rac1 expression.[33] These studies have highlighted the importance of Rac in controlling immunologic functions of DCs, T cells, or B cells through its ability to regulate actin-dependent cytoskeletal processes.[12,34,35] However, the fact that Rac expression was not altered in *Rras*$^{-/-}$ BM-DCs would suggest alternative mechanisms being involved. Future studies using gene expression profiling may identify R-Ras regulated genes that are critical for DC maturation.

BM-DCs lacking R-Ras have impaired LPS-induced surface up-regulation of CD86 and MHC class II. A possible explanation could be related to the role of R-Ras in vesicular trafficking. It has been reported that, although R-Ras is inactive on the plasma membrane, it is more active in endosomes.[36,37] Indeed, blocking R-Ras in PC12 cells significantly perturbs calcium-mediated exocytosis. It remains to be determined whether the observed decreased surface maturation markers in *Rras*$^{-/-}$ DCs are the result of an attenuated transport of these receptors from the endoplasmic reticulum to the plasma membrane.

Ligand binding to TLRs triggers the coupling of adaptor molecules, such as MyD88 and IRAKs, to the activation of 3 major signaling cascades, which include NF-κB, p38, and JNK.[38] Alternatively, LPS activates Akt in DCs through the PI3K signaling pathway.[39] These signaling pathways play critical roles in regulating DC maturation, endocytosis, cytokine production, gene expression, and survival. To our knowledge, the increase in GTP-bound R-Ras in response to TLR4 stimulation is the first demonstration that a member of the Ras subfamily can be activated by this receptor class in DCs. Indeed, the activation of the classic Ras was only observed 60 minutes after TLR4 stimulation. Akt has been shown to be important for DC maturation and survival.[40-43] Although unknown in immune cells, the ability of R-Ras in activating Akt has been extensively demonstrated in fibroblasts and epithelial cells, presumably through its interaction with the p110α subunit of PI3K.[44,45] Consistently, LPS-activated *Rras*$^{-/-}$ BM-DCs revealed reduced Akt activation. It was reported that PI3K regulates a negative feedback pathway limiting IL-12 production and curtailing excessive T_H1 polarization in DCs.[46] It will be of interest to investigate whether this negative feedback pathway is disrupted in *Rras*$^{-/-}$ DCs.

p38 MAPK signaling is critical for actin reorganization and MHC class II up-regulation during DC maturation,[11] whereas NF-κB is thought to be important for cytokine release.[47] The initial burst in endocytosis on LPS stimulation in DCs is p38 dependent, as treatment with the p38 inhibitor SB203580 inhibits this uptake.[11] In addition, p38 signaling is linked to DC adhesion and spreading,

as Vav1 was shown to be important in adhesion-dependent p38 activation. As reported previously, p38 is mapped upstream of Rap1 in J774.A1.[16,30] Thus, it is tempting to speculate a potential signaling pathway of R-Ras > p38 > Rap1 in regulating specific DC functions. Validating this hypothesis will require the demonstration of direct interaction between components of the TLR4 signaling pathway and R-Ras. Furthermore, as LPS-treated cells have increased complex formation between PI3K and components of the TLR4 signaling cascade, including MyD88 and TRAF6,[48] we hypothesize that R-Ras may also bind to members of this complex as well.

By live cell imaging techniques, we uncovered that LPS-activated *Rras*$^{-/-}$ DCs were impaired in forming immune synapses with naive T cells. Mechanistically, it is possible that R-Ras plays a positive role in synapse formation through either a direct or an indirect mechanism. For example, the failure of *Rras*$^{-/-}$ BM-DCs to spread on fibronectin is indicative of R-Ras having a positive role in modulating actin dynamics, as previously suggested.[49] It has been shown that DC dendrites could isotropically extend their cell body until they entangled a T cell and formed a stable DC–T-cell contact. Alternatively, the clustering of adhesion molecules, such as MHC class II, CD86, and CD40, at the c-SMAC and p-SMAC could be positively regulated by R-Ras. In this case, the reduction of these maturation markers on LPS-stimulated *Rras*$^{-/-}$ DCs might explain the impaired immune synapse formation. Our results are, however, contrary to studies of DCs from *Rac1/2*$^{-/-}$ mice. Although *Rac1/2*$^{-/-}$ DCs were significantly impaired in synapse formation, their maturation in response to LPS was normal.[12] Thus, it is tempting to speculate that R-Ras may act upstream of Rac in the hierarchy of TLR4 signaling. In conclusion, our results reveal previously unknown functions of R-Ras in DCs. By modulating the Akt and p38 signaling in response to TLR4 activation in DCs, R-Ras influences actin cytoskeleton-dependent processes and plays a role in immune synapse formation and mounting T-cell responses.

Acknowledgments

The authors thank Drs Thomas Moran, Gwendalyn Randolph, Adrian Ting, Jay Unkeless, Julie Blander, and Stuart Aaronson (Mount Sinai School of Medicine), Drs Bonnie Dittel and Demin Wang (Medical College of Wisconsin), and Dr Michael Dustin (New York University) for helpful advice; and Dr Rumana Huq (Microscopy Core, Mount Sinai) in assisting with live-cell imaging.

This work was supported by the National Institutes of Health (CA78509 and MH59771), Midwest Athletes Against Childhood Cancer (A.M.C.), Advancing a Healthier Wisconsin (A.M.C.), Wisconsin Breast Cancer Showhouse (A.M.C.), and the Children's Research Institute of the Children's Hospital of Wisconsin. G.S. was supported by the National Cancer Institute (predoctoral training grant T32CA078207).

Authorship

Contribution: G.S. designed experiments, conducted experimental procedures, analyzed the data, and wrote the manuscript; D.H., X.Y., J.H., P.J.Y.P., G.M., R.F.Q., and C.R.K. conducted experimental procedures and analyzed the data; and S.-H.C., M.M., and A.M.C. designed experiments, analyzed the data, and wrote the manuscript.

Conflict-of-interest disclosure: The authors declare no competing financial interests.

Correspondence: Andrew M. Chan, Department of Pediatrics, Division of Hematology and Oncology, Medical College of Wisconsin, 8701 Watertown Plank Rd, Milwaukee, WI 53226; e-mail: axchan@mcw.edu.

References

1. Steinman RM. Dendritic cells: understanding immunogenicity. *Eur J Immunol.* 2007;37(suppl 1): S53-S60.
2. Scheele JS, Marks RE, Boss GR. Signaling by small GTPases in the immune system. *Immunol Rev.* 2007;218:92-101.
3. Mitin N, Rossman KL, Der CJ. Signaling interplay in Ras superfamily function. *Curr Biol.* 2005; 15(14):R563-R574.
4. Li Y, Yan J, De P, et al. Rap1a null mice have altered myeloid cell functions suggesting distinct roles for the closely related Rap1a and 1b proteins. *J Immunol.* 2007;179(12):8322-8331.
5. Katagiri K, Ohnishi N, Kabashima K, et al. Crucial functions of the Rap1 effector molecule RAPL in lymphocyte and dendritic cell trafficking. *Nat Immunol.* 2004;5(10):1045-1051.
6. Kinashi T, Katagiri K. Regulation of lymphocyte adhesion and migration by the small GTPase Rap1 and its effector molecule, RAPL. *Immunol Lett.* 2004;93(1):1-5.
7. Pulecio J, Petrovic J, Prete F, et al. Cdc42-mediated MTOC polarization in dendritic cells controls targeted delivery of cytokines at the immune synapse. *J Exp Med.* 2010;207(12):2719-2732.
8. Kamon H, Kawabe T, Kitamura H, et al. TRIF-GEFH1-RhoB pathway is involved in MHC class II expression on dendritic cells that is critical for CD4 T-cell activation. *EMBO J.* 2006;25(17): 4108-4119.
9. Garrett WS, Chen LM, Kroschewski R, et al. Developmental control of endocytosis in dendritic cells by Cdc42. *Cell.* 2000;102(3):325-334.
10. West MA, Prescott AR, Eskelinen EL, Ridley AJ, Watts C. Rac is required for constitutive macropinocytosis by dendritic cells but does not control its downregulation. *Curr Biol.* 2000;10(14):839-848.
11. West MA, Wallin RP, Matthews SP, et al. Enhanced dendritic cell antigen capture via toll-like receptor-induced actin remodeling. *Science.* 2004;305(5687):1153-1157.
12. Benvenuti F, Hugues S, Walmsley M, et al. Requirement of Rac1 and Rac2 expression by mature dendritic cells for T cell priming. *Science.* 2004;305(5687):1150-1153.
13. Lowe DG, Capon DJ, Delwart E, Sakaguchi AY, Naylor SL, Goeddel DV. Structure of the human and murine R-ras genes, novel genes closely related to ras proto-oncogenes. *Cell.* 1987;48(1): 137-146.
14. Lowe DG, Goeddel DV. Heterologous expression and characterization of the human R-ras gene product. *Mol Cell Biol.* 1987;7(8):2845-2856.
15. Holly SP, Larson MK, Parise LV. The unique N-terminus of R-ras is required for Rac activation and precise regulation of cell migration. *Mol Biol Cell.* 2005;16(5):2458-2469.
16. Self AJ, Caron E, Paterson HF, Hall A. Analysis of R-Ras signalling pathways. *J Cell Sci.* 2001; 114(7):1357-1366.
17. Komatsu M, Ruoslahti E. R-Ras is a global regulator of vascular regeneration that suppresses intimal hyperplasia and tumor angiogenesis. *Nat Med.* 2005;11(12):1346-1350.
18. Delgado P, Cubelos B, Calleja E, et al. Essential function for the GTPase TC21 in homeostatic antigen receptor signaling. *Nat Immunol.* 2009; 10(8):880-888.
19. Kimmelman AC, Qiao RF, Narla G, et al. Suppression of glioblastoma tumorigenicity by the Kruppel-like transcription factor KLF6. *Oncogene.* 2004;23(29):5077-5083.
20. Lutz MB, Kukutsch N, Ogilvie AL, et al. An advanced culture method for generating large quantities of highly pure dendritic cells from mouse bone marrow. *J Immunol Methods.* 1999;223(1): 77-92.
21. Nunez Rodriguez N, Lee IN, Banno A, et al. Characterization of R-ras3/m-ras null mice reveals a potential role in trophic factor signaling. *Mol Cell Biol.* 2006;26(19):7145-7154.
22. Lin A, Schildknecht A, Nguyen LT, Ohashi PS. Dendritic cells integrate signals from the tumor microenvironment to modulate immunity and tumor growth. *Immunol Lett.* 2010;127(2):77-84.
23. Oinuma I, Ishikawa Y, Katoh H, Negishi M. The Semaphorin 4D receptor Plexin-B1 is a GTPase activating protein for R-Ras. *Science.* 2004; 305(5685):862-865.
24. Madrid LV, Mayo MW, Reuther JY, Baldwin AS Jr. Akt stimulates the transactivation potential of the RelA/p65 subunit of NF-kappa B through utilization of the Ikappa B kinase and activation of the mitogen-activated protein kinase p38. *J Biol Chem.* 2001;276(22):18934-18940.

25. Kinbara K, Goldfinger LE, Hansen M, Chou FL, Ginsberg MH. Ras GTPases: integrins' friends or foes? *Nat Rev Mol Cell Biol.* 2003;4(10):767-776.
26. Ueda H, Morishita R, Yamauchi J, Itoh H, Kato K, Asano T. Regulation of Rac and Cdc42 pathways by G(i) during lysophosphatidic acid-induced cell spreading. *J Biol Chem.* 2001;276(9):6846-6852.
27. Thrasher AJ, Burns SO. WASP: a key immunological multitasker. *Nat Rev Immunol.* 2010;10(3):182-192.
28. Burns SO, Killock DJ, Moulding DA, et al. A congenital activating mutant of WASp causes altered plasma membrane topography and adhesion under flow in lymphocytes. *Blood.* 2010;115(26):5355-5365.
29. Wozniak MA, Kwong L, Chodniewicz D, Klemke RL, Keely PJ. R-Ras controls membrane protrusion and cell migration through the spatial regulation of Rac and Rho. *Mol Biol Cell.* 2005;16(1):84-96.
30. Caron E, Self AJ, Hall A. The GTPase Rap1 controls functional activation of macrophage integrin alphaMbeta2 by LPS and other inflammatory mediators. *Curr Biol.* 2000;10(16):974-978.
31. Goldfinger LE, Ptak C, Jeffery ED, Shabanowitz J, Hunt DF, Ginsberg MH. RLIP76 (RalBP1) is an R-Ras effector that mediates adhesion-dependent Rac activation and cell migration. *J Cell Biol.* 2006;174(6):877-888.
32. Dustin ML. Modular design of immunological synapses and kinapses. *Cold Spring Harb Perspect Biol.* 2009;1(1):a002873.
33. Li H, Oliver T, Jia W, He YW. Efficient dendritic cell priming of T lymphocytes depends on the extracellular matrix protein mindin. *EMBO J.* 2006;25(17):4097-4107.
34. Savina A, Peres A, Cebrian I, et al. The small GTPase Rac2 controls phagosomal alkalinization and antigen crosspresentation selectively in CD8(+) dendritic cells. *Immunity.* 2009;30(4):544-555.
35. Walmsley MJ, Ooi SK, Reynolds LF, et al. Critical roles for Rac1 and Rac2 GTPases in B cell development and signaling. *Science.* 2003;302(5644):459-462.
36. Takaya A, Kamio T, Masuda M, et al. R-Ras regulates exocytosis by Rgl2/Rlf-mediated activation of RalA on endosomes. *Mol Biol Cell.* 2007;18(5):1850-1860.
37. Stasyk T, Schiefermeier N, Skvortsov S, et al. Identification of endosomal epidermal growth factor receptor signaling targets by functional organelle proteomics. *Mol Cell Proteomics.* 2007;6(5):908-922.
38. O'Neill LA. When signaling pathways collide: positive and negative regulation of toll-like receptor signal transduction. *Immunity.* 2008;29(1):12-20.
39. Ardeshna KM, Pizzey AR, Devereux S, Khwaja A. The PI3 kinase, p38 SAP kinase, and NF-kappaB signal transduction pathways are involved in the survival and maturation of lipopolysaccharide-stimulated human monocyte-derived dendritic cells. *Blood.* 2000;96(3):1039-1046.
40. Arron JR, Vologodskaia M, Wong BR, et al. A positive regulatory role for Cbl family proteins in tumor necrosis factor-related activation-induced cytokine (trance) and CD40L-mediated Akt activation. *J Biol Chem.* 2001;276(32):30011-30017.
41. Flaherty DM, Hinde SL, Monick MM, et al. Adenovirus vectors activate survival pathways in lung epithelial cells. *Am J Physiol Lung Cell Mol Physiol.* 2004;287(2):L393-L401.
42. Mattioli B, Giordani L, Quaranta MG, Viora M. Leptin exerts an anti–apoptotic effect on human dendritic cells via the PI3K-Akt signaling pathway. *FEBS Lett.* 2009;583(7):1102-1106.
43. Park D, Lapteva N, Seethammagari M, Slawin KM, Spencer DM. An essential role for Akt1 in dendritic cell function and tumor immunotherapy. *Nat Biotechnol.* 2006;24(12):1581-1590.
44. Osada M, Tolkacheva T, Li W, et al. Differential roles of Akt, Rac, and Ral in R-Ras-mediated cellular transformation, adhesion, and survival. *Mol Cell Biol.* 1999;19(9):6333-6344.
45. Marte BM, Rodriguez-Viciana P, Wennstrom S, Warne PH, Downward J. R-Ras can activate the phosphoinositide 3-kinase but not the MAP kinase arm of the Ras effector pathways. *Curr Biol.* 1997;7(1):63-70.
46. Fukao T, Tanabe M, Terauchi Y, et al. PI3K-mediated negative feedback regulation of IL-12 production in DCs. *Nat Immunol.* 2002;3(9):875-881.
47. Kaisho T, Tanaka T. Turning NF-kappaB and IRFs on and off in DC. *Trends Immunol.* 2008;29(7):329-336.
48. Dauphinee SM, Karsan A. Lipopolysaccharide signaling in endothelial cells. *Lab Invest.* 2006;86(1):9-22.
49. Al-Alwan MM, Rowden G, Lee TD, West KA. The dendritic cell cytoskeleton is critical for the formation of the immunological synapse. *J Immunol.* 2001;166(3):1452-1456.